The generalized Proudman-Johnson equation at large Reynolds numbers

Sun-Chul Kim* and Hisashi Okamoto†

August 23, 2011

Abstract

We consider the generalized Proudman-Johnson equation with an external force. Solving its steady-states numerically, we demonstrate that a unimodal pattern appears at large Reynolds numbers if and only if the parameter endowed in the equation is equal to unity. This may be interpreted as a strong connection of unimodal patterns to the two-dimensional Navier-Stokes equations.

1 Introduction

It is generally plausible that a simple input produces a simple output while a complex input results in a complex outcome in differential equations with an external forcing. Suppose for instance that we are given a second order linear differential equation with a sinusoidal force,

$$-u'' + au = \sin nx \qquad (-\pi < x < +\pi) \text{ with the periodic boundary condition,}$$

where $a > 0$ is a constant and n is a positive integer. The right hand side of this equation, $\sin nx$, is regarded as an input. The solution, regarded as an output, is

$$u = \frac{\sin nx}{n^2 + a},$$

which oscillates exactly the same times as the driving force. In other words, the mode of the output coincides with that of the input. If a depends on x but is close to a constant, the moduli of the Fourier coefficient of $\sin nx$ (and/or $\sin(n \pm 1)x$) are much larger than those of other coefficients. Accordingly, the number of oscillation of u (or lap number) is the

*Department of Mathematics, Chung-Ang University, 221 Heukseok-dong, Dongjak-ku, Seoul 156-756 Korea. Supported by Basic Science Research Program through the National Research Foundation of Korea funded by the Ministry of Education, Science and Technology(2010-0007654).

†Research Institute for Mathematical Sciences, Kyoto University, Kyoto 606-8502 Japan. Partially supported by JSPS Grant 20244006

same as that of the input. As far as we know, there is no special reason to doubt of such a principle in any linear or weakly nonlinear equation of constant coefficients except in the case of resonance.

It was therefore a surprise for us to find that the two-dimensional (2D) Navier-Stokes equations possess a solution of very simple character (single peak solution) at high Reynolds numbers, despite the fact that they are driven by a force of many oscillation: See Kim & Okamoto (2010). The solutions oscillate as many times as the driving force if the Reynolds number is small, but the stream function has one and only one peak if the Reynolds number is large enough. We called such a solution unimodal. To be precise, our claim is that among many steady-states there exists at least one unimodal solution if the Reynolds number is large enough—thus, non-unimodal solutions may co-exist with a unimodal solution. For example, the rhombic flow considered in Kim & Okamoto (2003) produces many bifurcating solutions but there is always a unimodal solution if the Reynolds numbers is large.

We suspected in Kim & Okamoto (2010) that this phenomenon is closely related to 2D incompressible flows and that it does not appear in other equations such as reaction-diffusion equations. The inverse cascade theory of 2D turbulence may be related to the appearance of the single pair of large vortices in Kim & Okamoto (2010). However, because of the computational difficulty of the Navier-Stokes flows at high Reynolds numbers, we could not supply in Kim & Okamoto (2010) enough materials for demonstrating this conjecture. It is the aim of the present paper to verify this phenomena in a simple model of 2D incompressible Navier-Stokes equations which we call the generalized Proudman-Johnson equation.

The generalized Proudman-Johnson equation was proposed by Okamoto & Zhu (2000) in order to study the role of convection term in the blow-up problem. An equation equivalent to it had appeared earlier in Budd *et al.* (1994). Here we study it in view of the pattern formation. It is written as

$$\psi_{txx} + \psi\psi_{xxx} - \alpha\psi_x\psi_{xx} = \frac{1}{R}\left(\psi_{xxxx} - f\right), \tag{1.1}$$

where α is a real parameter and R is a positive parameter, which we call the Reynolds number.

This equation unifies many differential equations. In fact, if $\alpha = -(m-3)/(m-1)$, then any solution of (1.1) produces an exact, self-similar solution of the Navier-Stokes equations in $\mathbb{R}^m$. In particular, the equation with $\alpha = 1$ (i.e. $m = 2$) gives us the original Proudman-Johnson equation which was derived in Proudman & Johnson (1962). Also, the three-dimensional (3D) exact solution for the Navier-Stokes equations are obtained with $\alpha = 0$. If $\alpha = -3$, (1.1) is the Burgers equation. To see this, we differentiate $\psi_t + \psi\psi_x = \frac{1}{R}\psi_{xx}$ twice to obtain (1.1) with $\alpha = -3$ and without external force. The equation with $\alpha = -2$

is obtained if we differentiate the Hunter-Saxton equation (Hunter & Saxton, 1991) which can be written as $\psi_{tx} + \psi\psi_{xx} + \frac{1}{2}(\psi_x)^2 = \frac{1}{R}\psi_{xxx}$. See Okamoto (2009) and Okamoto & Zhu (2000). Other applications can be found in Budd *et al.* (1993)&(1994), Saxton & Tiğlay (2008), and the references therein. The equation (1.1) also appears in Holm *et al* (2008) when $\nu = 0$. There, the authors study the motion of water waves.

The case of $\alpha = \infty$ is of some interest. If we set $\psi = \varphi/\alpha$ and $f \equiv 0$, and if we let $\alpha \to \infty$, then we obtain $\varphi_{txx} - \varphi_x\varphi_{xx} = R^{-1}\varphi_{xxxx}$. After integrating this in x and setting $\varphi_x = 2u$, we have

$$u_t = u_{xx} + u^2 - \gamma,$$

where γ depends only on t. This equation, together with the constraint $\int_{-\pi}^{+\pi} u(t,x)\,\mathrm{d}x = 0$, was studied in Budd *et al.* (1993), Budd *et al.* (1994), Ikeda *et al.* (2003), Ikeda *et al.* (2001), and Okamot & Zhu (2000) in the context of blow-up of solutions. Interesting applications of (1.1) with $\alpha = 1$ can be found in Cox (1991), Cox (1991a), Grundy & McLaughlin (1997), and Grundy & McLaughlin (1999). The blow-up problem is considered in Budd *et al.* (1994), Chen & Okamoto (2002), and Okamoto & Zhu (2000).

With $\alpha = 1$ and $f = \sin\ell x$ with $\ell = 2, 3$, we showed in Kim & Okamoto (2010) numerically that nontrivial solutions bifurcate from the trivial solution $\ell^{-4}\sin\ell x$. We found that, if R is not large, the solution has ℓ peaks. As the Reynolds number R tends to ∞, one family of the solutions tends to be unimodal. Specifically, the solution tends to a constant times $\sin x$, although the system is forced by $\sin 2x$ or $\sin 3x$. We may therefore say that at very large Reynolds numbers, a solution shows a topologically simple, universal pattern, irrespective of the mode of the forcing. We also conjectured in Kim & Okamoto (2010) that this pattern occurs only in differential equations related to the 2D Navier-Stokes equations.

Now one may naturally wonder if such a peculiar bifurcation is common or not, generic or not. In dynamical systems's words, we may wonder if such a case is structurally stable or not. We wish therefore to embed the equation into a more general equation (or a system of equations). The equation (1.1) seems to be a good candidate because of the properties stated above. We have thus been led to the problem to study how the bifurcating structure in (1.1) may change as α varies. Our computation below demonstrates that the unimodality do not occur if $\alpha > 1$. In particular, the occurrence of the unimodal solution is structurally unstable. Also, we observe no change from many modes to single mode as $R \to \infty$ in the case of axi-symmetric solutions of the Navier Stokes equations in dimension ≥ 3, or in the Burgers equation.

Remark. The reader may wonder why we impose an external force of the form $\frac{1}{R}f$.

Indeed we may consider

$$\phi_{txx} + \phi\phi_{xxx} - \alpha\phi_x\phi_{xx} = \frac{1}{R}\phi_{xxxx} - f$$

as well, but this is mathematically equivalent to (1.1). In fact, if we change variables as

$$(\phi, t) \mapsto (R\psi, R^{-1}t),$$

and then replace R^2 by R, i.e., re-define the Reynolds number, then we obtain (1.1).

The present paper is organized as follows. The numerical method is described in section 2. Results in the case of $\alpha = 1$ are presented in section 3. Numerical results in the case of $\alpha > 1$ are presented in section 4. The cases of $-3 < \alpha < 1$, $\alpha = -3$, and $-\infty < \alpha < -3$ are studied in section 5, 6, and 7, respectively. Critical Reynolds numbers are determined in section 8. Conclusions are given in section 9. Section 10 is an appendix, where we will show that qualitatively the same result is obtained for a different external force.

2 Discretization by the spectral method

Henceforth we consider steady-states of (1.1) with the periodic boundary condition. In order to eliminate the translational indefiniteness (i.e., if $\psi(x)$ is a solution, then $\psi(x-c)$ with a constant c is a solution, too.), we restrict ourselves to solutions which are odd functions.

We require that $\psi(x) = \ell^{-4}\sin\ell x$, which we call a trivial solution, is a solution of (1.1). This is equivalent to set

$$f = \sin\ell x - \frac{(\alpha-1)R}{2\ell^5}\sin(2\ell x). \tag{2.1}$$

If we integrate (1.1) in x, we have

$$\frac{1}{R}\psi''' + \frac{1}{R\ell}\cos(\ell x) - \frac{\alpha-1}{4\ell^6}\cos(2\ell x) - \psi\psi'' + \frac{\alpha+1}{2}(\psi')^2 = \text{constant}. \tag{2.2}$$

Let

$$\psi^N = \sum_{n=1}^{N} a_n \sin nx \tag{2.3}$$

be an approximation. Substituting this into (2.2), we expand the left hand side of (2.2) into cosine series. For $k = 1, 2, \cdots, N$ we set as $F_k(R, \alpha; a_1, a_2, \cdots, a_N)$ the coefficient of $\cos kx$ in the equation above. Then, we obtain after some calculations

$$\begin{aligned} F_k(R, \alpha; a_1, a_2, \cdots, a_N) = &-\frac{k^3}{R}a_k + \frac{1}{R\ell}\delta_{k,\ell} - \frac{\alpha-1}{4\ell^6}\delta_{k,2\ell} \\ &+ \frac{1}{2}\sum_{m=1}^{N-k}\left[m(m+k)(\alpha+3) + k^2\right]a_m a_{m+k} - \frac{1}{4}\sum_{m=1}^{k-1}\left[m(m-k)(\alpha+3) + k^2\right]a_m a_{k-m}, \end{aligned}$$

where $\delta_{k,j} = 1$ if $k = j$, and $\delta_{k,j} = 0$ otherwise. $F = (F_1, F_2, \cdots, F_N)$ defines a mapping from $(0, \infty) \times \mathbb{R} \times \mathbb{R}^N$ into $\mathbb{R}^N$. We compute zeros of F by the path-continuation method, see Kim & Okamoto (2010). With $N = 200$, most of the solutions were easily computed for $R < 5000$. For larger R we used $N = 500$ or $N = 1000$. As a test for convergence, we employed the following criterion:

$$\frac{\|\psi^N - \psi^{2N}\|}{\|\psi^N\|} < 10^{-3},$$

where $\|\cdot\|$ is the L^2-norm and ψ^N denotes the approximate solution (2.3) with mode N. We increased N until this criterion was satisfied.

If $\alpha \neq 1$, then the force f in (2.1) consists of two terms of different order. Accordingly, the reader may wonder if it is a dimensionally correct choice. We therefore compute solutions in the case where f is given by $f = \sin \ell x$. In this case we do not have an explicit trivial solution, but we can still compute in the same way. The result, which will be shown in section 10, turns out to be qualitatively the same.

3 Results in the case of $\alpha = 1$

We first recall some results in Kim & Okamoto (2010), where the case of $\alpha = 1$ was studied with $\ell = 2$ and $\ell = 3$. The bifurcation diagrams are reproduced here as Figure 1. We noticed numerically that

Proposition 3.1 *There exists a family of solutions ψ_R for a sufficiently large R which satisfies $\lim_{R\to\infty} \psi_R = \ell \sin x$.*

The profiles of the first order derivatives ψ', which are plotted in Figure 2, look similar to the trivial solution if they are close to the bifurcation point. However, they have one and only one peak if they are far enough from the trivial solution. See Figure 2. In Kim & Okamoto (2010) we also presented an asymptotic analysis by which we can expect $\lim_{R\to\infty} \psi_R = \ell \sin x$. The system is driven by $\sin \ell x$. Nevertheless, the steady-states which are proportional to $\sin x$ are realized when $R \gg 1$. Since those solutions have one and only one peak, we called them *unimodal*.

Now since we verified Proposition 3.1 only in the case of $\ell = 2$ and 3, the reader may wonder if it is always true for an arbitrary ℓ. In the present paper, we continued numerical experiments with larger ℓ's and confirmed Proposition 3.1 for $4 \leq \ell \leq 10$. Some numerical results are as follows:

Figure 3 is the bifurcation diagram in the case of $\ell = 4$. A family of solutions bifurcates from the trivial solution $\psi = 4^{-4} \sin 4x$, which are represented by the horizontal axis in

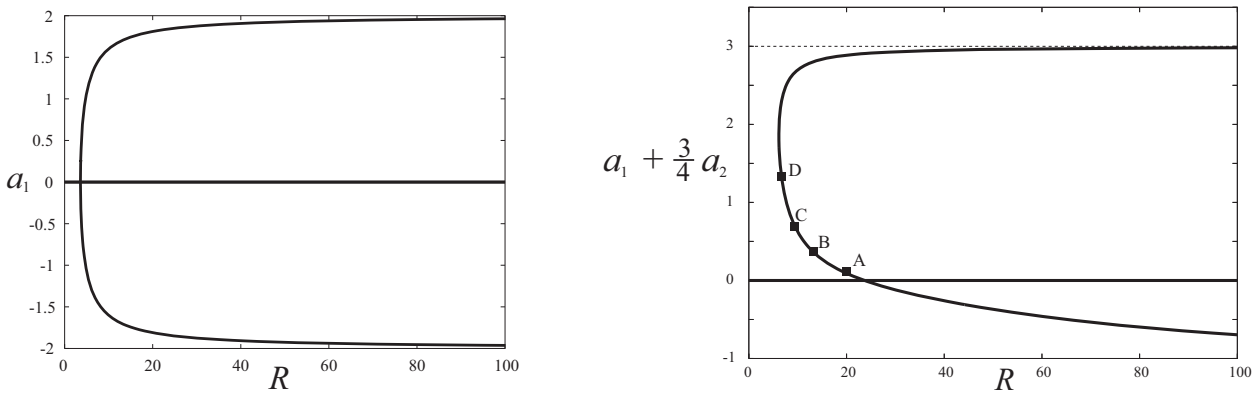

Figure 1: Bifurcation diagrams $\alpha = 1$. $\ell = 2$ (left). $\ell = 3$ (right).

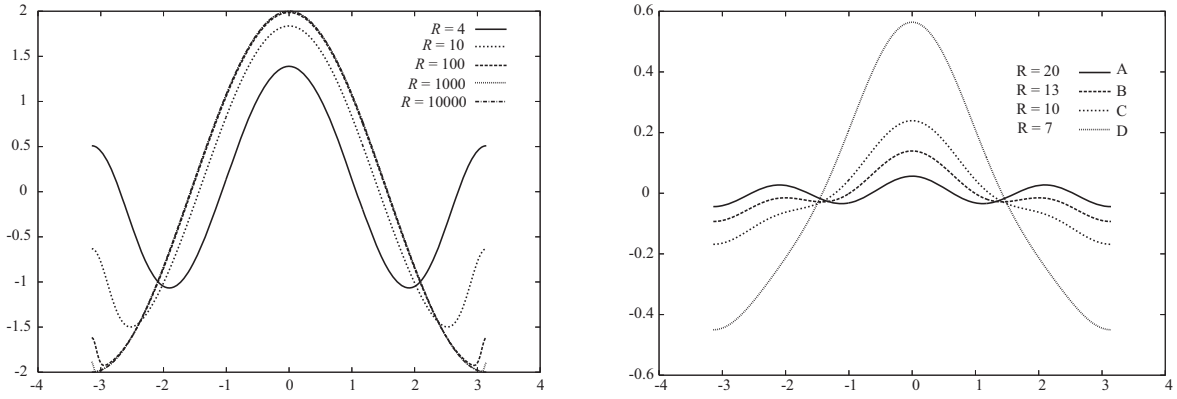

Figure 2: Profiles of ψ'. $\ell = 2$, $\alpha = 1$. $R = 4, 10, 100, 1000, 10000$ (left). $\ell = 3$, $\alpha = 1$, $R = 7, 10, 13, 20$. These solutions correspond to the black squares in Figure 1 (right).

Figure 3. They bifurcate at around $R \approx 81$. It is a subcritical pitchfork bifurcation. After experiencing a turning point which is located at around $R \approx 7.5$, they continue to exist in $7.5 < R < \infty$ with no further bifurcation. Figure 4 shows the graphs of ψ' with various R. The one near the bifurcation point ($R = 70$) has four peaks, while those away from the trivial solution have one and only one peak. As Figure 3 shows, the diagram has the lines $a_1 = \pm 4$ as an asymptote. In fact the solutions are asymptotically $\psi \to \pm 4 \sin x$ as $R \to \infty$. Table 1 is the list of the Fourier coefficients of a solution with $R = 10000$. Obviously, they are very small except for a_1, which is close to 4. (The other solution is nothing but $\psi(x+\pi)$.)

Here is a remark about the diagram. If ℓ is even the equation is symmetric with respect to $f(x) \mapsto f(x+\pi)$. Therefore, if the bifurcation diagram is drawn in (R, a_1), then they are symmetric with respect to the horizontal axis. On the other hand, if ℓ is odd, there is no such symmetry. This symmetry induces a fact that the bifurcation from the trivial solution is a pitchfork if ℓ is even, while it is transcritical if ℓ is odd.

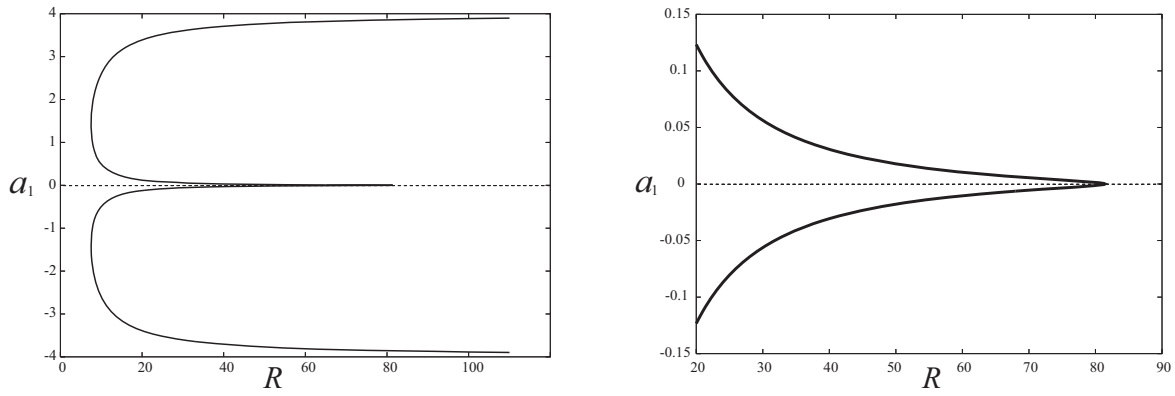

Figure 3: The bifurcation diagram. $\ell = 4$. $\alpha = 1$. The horizontal axis (the broken line) denotes trivial solutions. The vertical axis represents a_1, the coefficient of $\sin x$ (left). The part near the bifurcation point is magnified in the right.

Table 1: Fourier coefficients of the solution at $R = 10000$. $\ell = 4$.

coefficients	
a_1	3.99887570831577
a_2	0.00002222222222
a_3	0.00000000054426
a_4	0.00000088889289
a_5	-0.00000034718202

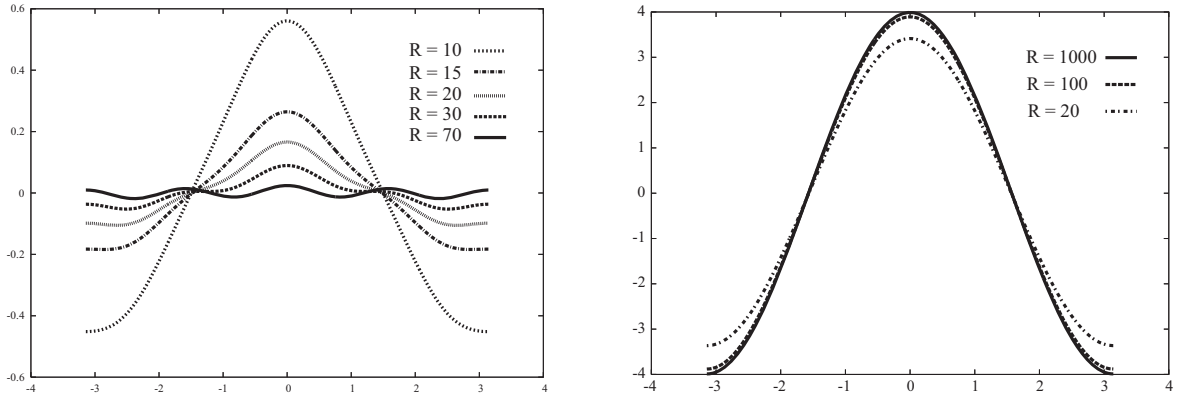

Figure 4: Profiles of ψ'. $\ell = 4$. $\alpha = 1$. $R = 10, 15, 30, 70$ (left). $R = 20, 100, 1000$ on uppermost branch (right). The figure on the right shows that $\lim_{R\to\infty} \psi'_R = 4\cos x$.

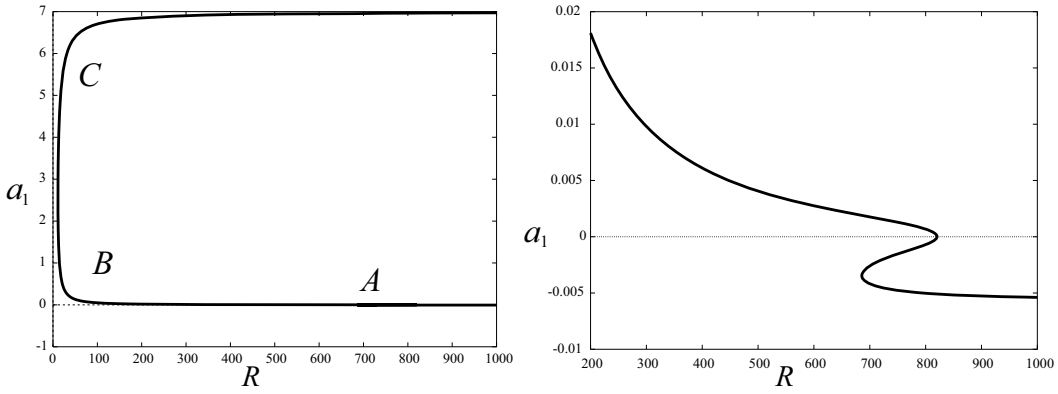

Figure 5: Bifurcation diagrams. $\ell = 7$. $\alpha = 1$. The graph on the right is the blow-up of the one on the left near the bifrucation point. The meaning of the letters A, B, C are explained in Figure 6.

Table 2: Fourier coefficients of the solution at $R = 10000$. $\ell = 7$.

coefficients	
a_1	6.99710851254874
a_2	0.00002222222222
a_3	0.00000000031111
a_4	0.00000088888890
a_5	0.00000000007881
a_6	0.00000016326531
a_7	0.00000000003563

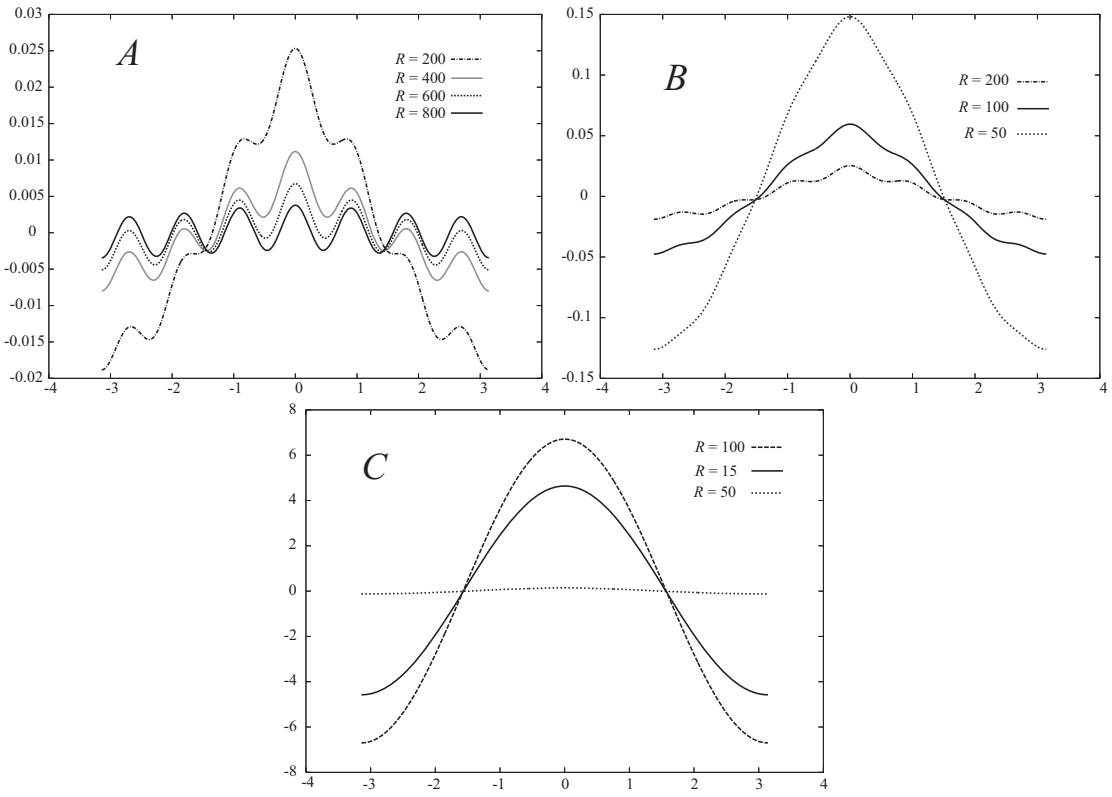

Figure 6: Profiles of ψ'. $\ell = 7$. $\alpha = 1$. The graphs in the upper right (labelled as A) are those which are close to the bifurcation point. The letters A, B, C imply that the solutions correspond those in the area indicated by the same letter in Figure 5.

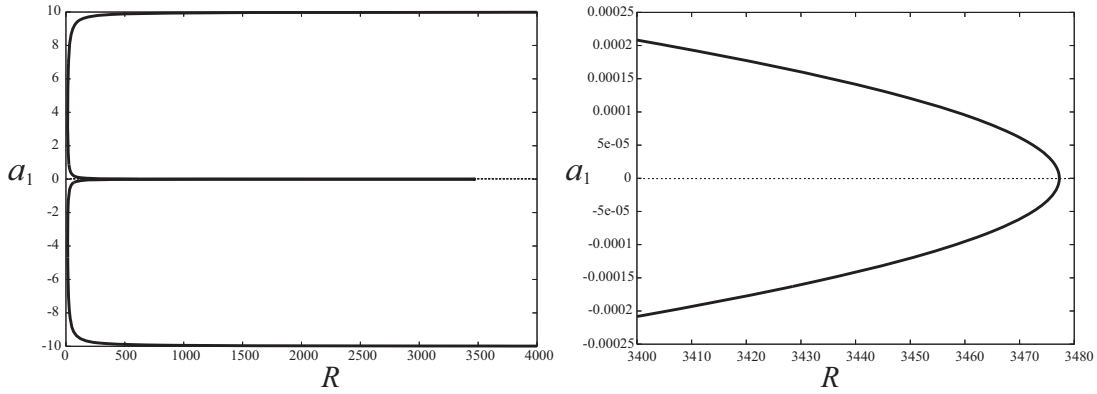

Figure 7: Bifurcation diagrams. $\ell = 10$. $\alpha = 1$.

Other cases are seen in Figures 5, 6, and 7, which may serve as evidence supporting Proposition 3.1 for $4 \le \ell \le 10$. We also provided a very plausible argument in p.66 in Kim & Okamoto (2010) for the validity of this proposition. We, however, do not know a mathematical proof.

Since $0.0000222\cdots \approx \frac{2}{9} \div 10000$, Tables 1 and 2 suggest that $a_1 \approx \ell$ and $a_2 \approx \frac{2}{9R}$ as $R \to \infty$. This is confirmed by the following asymptotic analysis. We showed in Kim & Okamoto (2010) that the following expansion is plausible

$$\psi(x) = \ell \sin x + \frac{h_1(x)}{R} + o\left(\frac{1}{R}\right) \qquad (R \to \infty),$$

where $h_1(x)$ is to be determined. We start with this and substitute this into (1.1). We then collect the R^{-1} terms, which turn out to be

$$\ell \left(\sin x \frac{d}{dx} - \cos x\right) \left(\frac{d^2}{dx^2} + I\right) h_1(x) - \ell \sin x + \sin \ell x = 0, \tag{3.1}$$

where I denotes the identity operator. Putting $h_1(x) = \sum_{k=1}^{\infty} c_k \sin kx$ and substituting this into (3.1), we obtain

$$\sin \ell x - \ell \sin x + \frac{\ell}{2} \sum_{k=1}^{\infty} c_k (k^2 - 1) \left[(k+1)\sin(k-1)x - (k-1)\sin(k+1)x\right] = 0.$$

If $\ell > 3$, this equation gives us

$$\ell \left(-1 + \frac{9}{2} c_2\right) = 0, \quad 16\ell c_3 = 0, \quad \ell \left(-\frac{3}{2} c_2 + \frac{75}{2} c_4\right) = 0. \tag{3.2}$$

In particular, we have $c_2 = 2/9 = 0.2222\cdots$, $c_3 = 0$, and $c_4 = c_2/25 = 0.00888\cdots$. Now this agrees perfectly with numerical data in Tables 1 and 2.

Before going into the study of the cases of $\alpha \neq 1$, we present here a graph of neutral curves—the curves of critical Reynolds numbers as a functions of α. For a fixed α, the trivial solution is stable for small R. We derived the linearized operator at the trivial solution and computed its eigenvalues. The linearised operator is derived in the function space of odd functions. In other words, only perturbations by $\sin kx$ ($k = 1, 2, \cdots$) are considered. By the bisection method, we compute R^* such that the linearized operator at $R = R^*$ possesses 0 as an eigenvalue. This was computed with $N = 200$. Numerical outputs are compared with those with $N = 500$ and we verified that change in any case was smaller than 0.001. The results are drawn in Figure 8. As the left figure shows, two vertical lines $\alpha = -3.5$ and $\alpha = 1$ are asymptotes in the case of $\ell = 1$. Accordingly, the bifurcation from the trivial solution occurs if $-\infty < \alpha < -3.5$ or $1 < \alpha < +\infty$. In the case of $\ell = 2$, it occurs if $-\infty < \alpha < -3$ or $\alpha^* < \alpha < +\infty$.

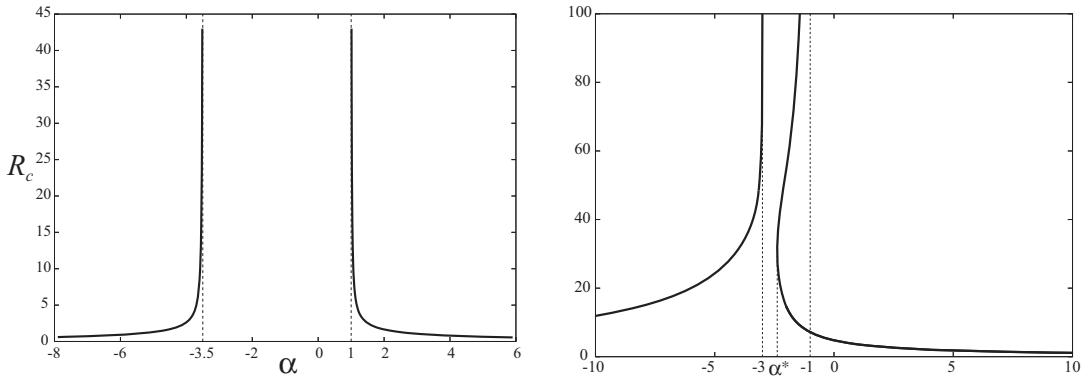

Figure 8: Critical Reynolds numbers for $\ell = 1$ and $\ell = 2$. The figure on the left hand side is the case of $\ell = 1$. Two vertical lines $\alpha = -3.5$ and $\alpha = 1$ are asymptotes. No bifurcation point was found in $-3.5 \leq \alpha \leq 1$. The figure on the right hand side is the case of $\ell = 2$. The line $\alpha = -3$ is an asymptote. The neutral curve on the right has a minimum α at $\alpha^* \approx -2.378$. It tends to upward indefinitely. It passes through $(\alpha, R) = (-1.433 \cdots, 100)$ and $(\alpha, R) = (-1.032, 1000)$. The asymptote seems to be $\alpha = -1$. We found no bifurcation point in $-3 \leq \alpha < \alpha^*$.

4 The case where $\alpha > 1$

From this section onward we consider the case of $\ell = 2$ and $\alpha \neq 1$. In the present section we show that there is no bifurcating branch with $R \to \infty$ if $\alpha > 1$.

Bifurcation diagrams in the case of $\alpha > 1$ are very different from those with $\alpha = 1$. See Figure 9. If $\alpha = 1$, the pitchfork extends to $R = \infty$. However, if $\alpha > 1$, a solution branch for all the fixed $\alpha \in (1, \infty)$ has an upper bound $R_0(\alpha)$ such that all the solutions bifurcating from the trivial solution satisfies $R \leq R_0(\alpha)$. We do not know why such a difference suddenly appears when α exceeds 1.

This character of the bifurcation diagram is observed in each of our experiment in the case of $\alpha > 1$. Figure 10 shows the cases of $1.08 \leq \alpha \leq 5$. There is no solution with $R \to \infty$. Instead, there is a branch in which R tends to zero and $|a_1|$ tends to infinity.

Just to make it sure, we studied the profiles of ψ as $R \to 0$. The solutions diverge in the order of R^{-1}. We therefore plotted profiles of $R\psi'''$ in Figure 11, which then suggests that $\lim_{R \downarrow 0} R\psi'''$ exists but the limit function is not a constant multiple of $\cos x$. Therefore no unimodality is observed in this case.

5 The case where $-3 < \alpha < 1$

We now consider the case where $\ell = 2$ and $-3 < \alpha < 1$.

For a fixed $-1 \leq \alpha \leq 1$, we obtained a pitchfork bifurcation, as is drawn in Figure 12.

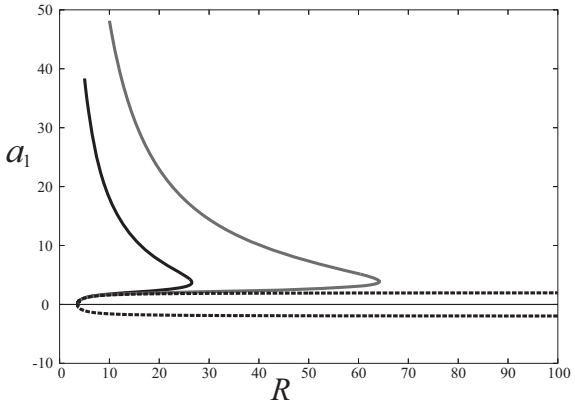

Figure 9: Bifurcation diagrams. $\ell = 2$. $\alpha = 1, 1.002, 1.005$. The broken line is the diagram when $\alpha = 1$. The solid black line, $\alpha = 1.005$. The solid gray line, $\alpha = 1.002$. Those solutions with $a_1 < 0$ are omitted.

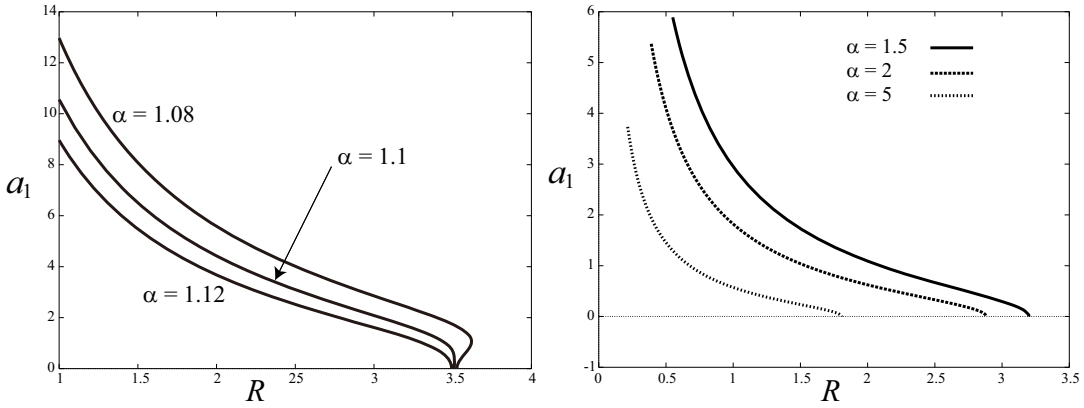

Figure 10: Bifurcation diagrams. $\ell = 2$. $\alpha = 1.08, 1.1, 1.12$ (left). $\alpha = 1.5.2.5$ (right).

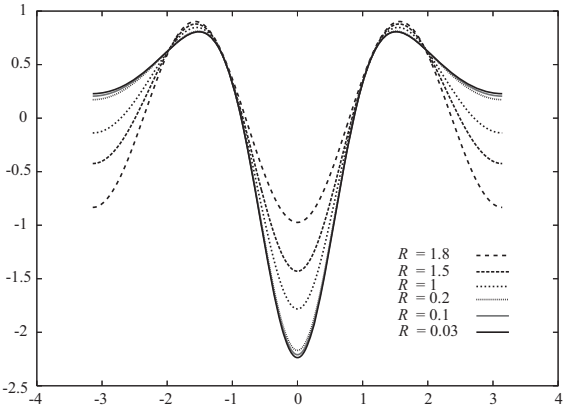

Figure 11: Profiles of $R\psi'''$. $\ell = 2, \alpha = 5$. $R = 0.03, 0.1, 1, 1.5, 1.8$.

This shows that, as α decreases, the bifurcating solution tends to the trivial solution and the bifurcation point moves to the right. However, the topology of the diagram is identical with that in the case of $\alpha = 1$.

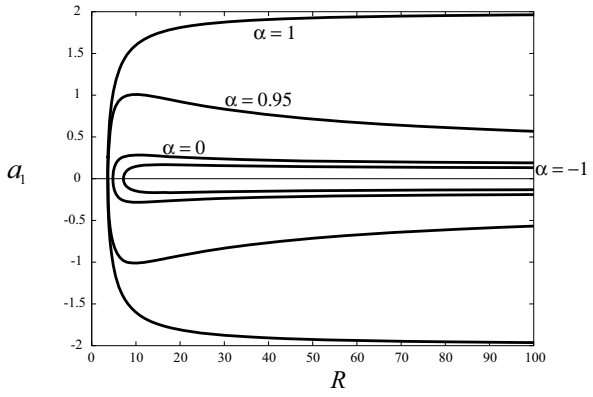

Figure 12: Bifurcation diagrams. $\ell = 2$. $\alpha = 1, 0.95, 0, -1$. The horizontal axis denotes trivial solutions. The vertical axis represents a_1, the coefficient of $\sin x$.

On the other hand, the bifurcation diagram looks substantially different if $\alpha < -1$. See Figures 13 and 14, for the case of $\alpha = -2, -2.25, -2.27$, respectively. They show that the second pitchfork, which has a larger critical Reynolds number, appears if $\alpha < -1$. This complies with Figure 8.

If $\alpha \leq -2.27$, then the diagram is disconnected as in Figure 14, which contains two hairpin curves in $193.7\cdots \leq R$ in addition to a closed loop in $21 < R < 94$. The loop is connected with the trivial solutions by two pitchfork points. The hairpin curves move rightwards as α decreases further. The size of the loop on the left hand side decreases as α decreases. Eventually all the solutions, except for the trivial solution, disappear. Some loops of the diagram are shown in Figure 14(right).

We now fix R and draw a bifurcation diagram in (α, a_1) plane. The diagram of the solutions for $R = 10$ is drawn in Figure 15. When $R = 100$, two turning points (the limit points) appear in the bifurcation diagram, see Figure 16. If we increase R further, the tips around $\alpha \approx -2.23$ become sharper, and computation becomes more difficult. See Figure 17, where only the part of $a_1 > 0$ is plotted.

As Figures 16 and 17 show, the diagram varies quite sensitively near $\alpha \approx 1$, although they in fact change continuously. The slope at $\alpha = 1$ is extremely large. This remarkable fact is a first indication that $\alpha = 1$ is very special, and is better understood when we consider them together with solutions of $\alpha > 1$.

We now study qualitatively the graphs of the solutions and examine if unimodality appears or not. Before going into detail, we first note that the concept of unimodality is not

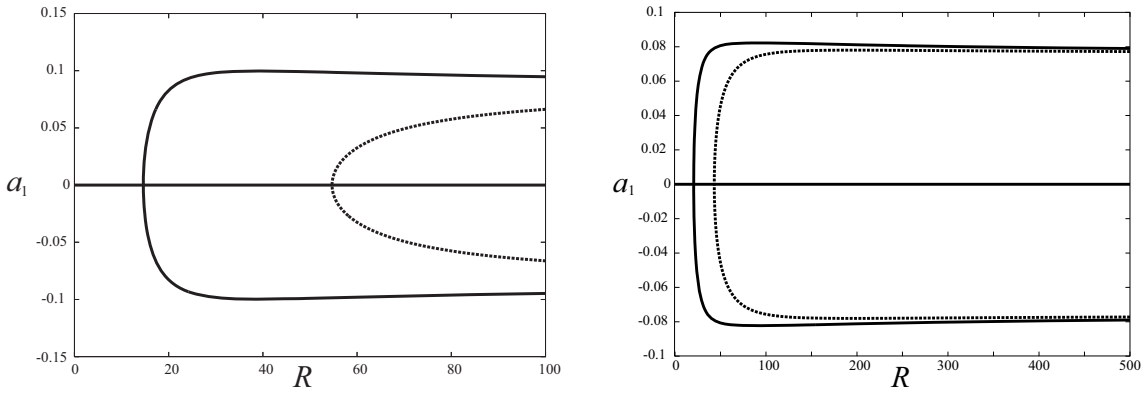

Figure 13: Bifurcation diagrams. $\ell = 2$. $\alpha = -2$ (left) and $\alpha = -2.25$ (right). In both cases two pitchforks bifurcate from the trivial solutions.

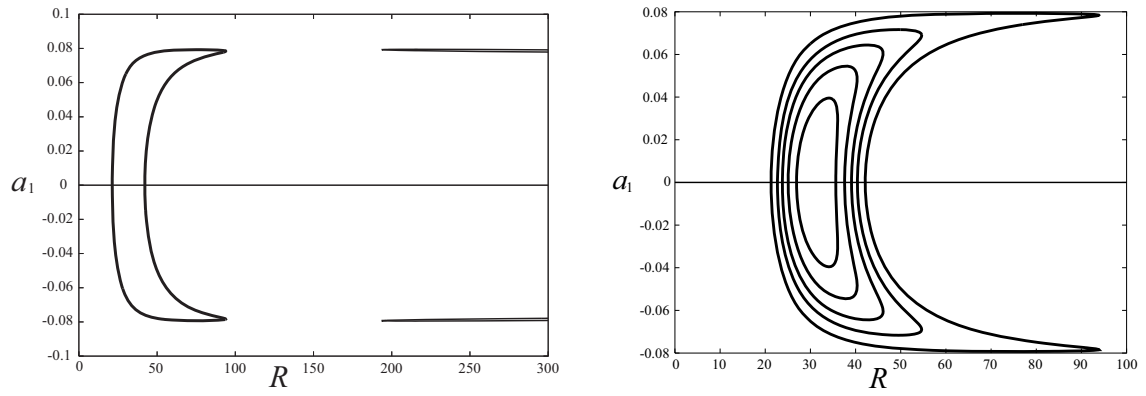

Figure 14: Bifurcation diagrams. $\ell = 2$. $\alpha = -2.27$ (left). Loops of solutions (right), where α is $-2.27, -2.3, -2.32, -2.34, -2.36$, respectively from the outermost to the innermost.

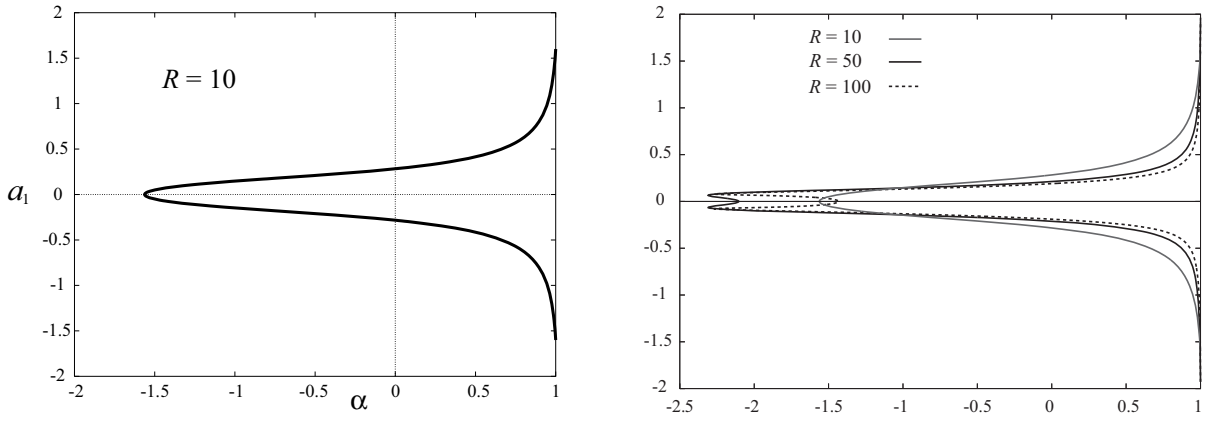

Figure 15: The bifurcation diagram: $\ell = 2$. $R = 10$ (left). $R = 10, 50, 100$ (right). The horizontal axis denotes the trivial solution. The vertical axis represents a_1.

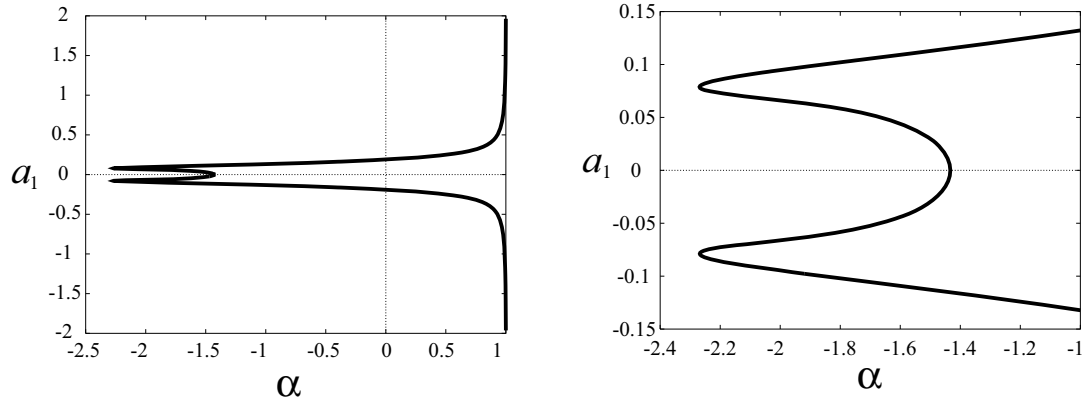

Figure 16: The bifurcation diagram: $\ell = 2$. $R = 100$.

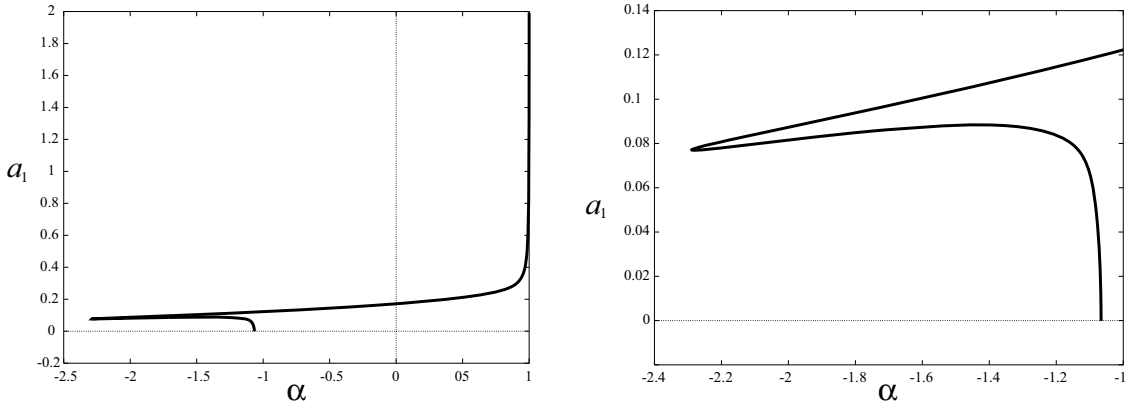

Figure 17: The bifurcation diagram when $\ell = 2, R = 500$.

free from ambiguity. In fact, there may be a case where ψ has a unique local maximum and a unique local minimum but its derivative, say ψ''', has more than one local maximum (and minimum). Accordingly, having one-peak or not depends on which derivative of the function we see. For instance, consider $\psi = \sin x + 0.1 \sin 3x$. The graph of ψ has one and only one peak in $-\pi < x \leq \pi$. However, $\psi''' = -\sin x - 2.7 \sin 3x$ has three peaks there.

Now the solutions with $\alpha = 1$ and $1 \ll R$ were *strongly unimodal*, by which we mean that derivatives of all order converge to a constant multiple of $\sin x$ or $\cos x$ as $R \to \infty$. In contrast to this, the *weak unimodality* such as in $\psi = \sin x + 0.1 \sin 3x$ does happen in the case of the generalized Proudman-Johnson equation. The situation is illustrated in Figure 18. At $\alpha = 1$ and $R = 10^4$, the solution ψ is very close to $2 \sin x$. And ψ', ψ'', ψ''' are very close to $2 \cos x, -2 \sin x, -2 \cos x$, respectively. On the other hand, if $\alpha = 0$ and $R = 10^5$, ψ and ψ' have one and only one local minimum, while ψ'' and ψ''' do have more than one local maximum (and minimum). The case of $\alpha = -1$ is shown in Figure 19 (left). Here we can see a very sharp transition layer (an internal layer) in ψ''' at $x = \pm\pi$. Transition layers also appear in the two solutions of $\alpha = -2$, see Figure 19 (right). In this case, transition layers appear in ψ''.

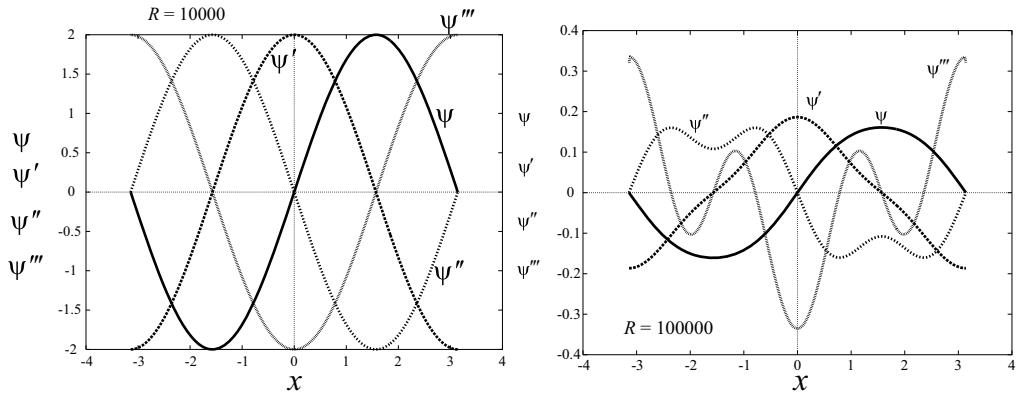

Figure 18: Graphs of $\psi, \psi', \psi'', \psi'''$. $\ell = 2$. $\alpha = 1, R = 10^4$(left). $\alpha = 0, R = 10^5$(right).

When $\alpha = 0$, the solutions represent steady-states of the 3D Navier-Stokes equations. Hence it would be interesting to see if a solution shows unimodality for large R. Figure 18 (right) and Figure 20 are the results. It shows no unimodality of ψ'''. Our computation suggests that $\lim_{R\to\infty} \psi$ exists but the limit function is not a constant multiple of $\sin x$. In fact, the Fourier coefficients a_k tends to zero if k is even, and to non-zero value if k is odd. This is reflected in the fact that ψ''' has four local maxima and minima. Consequently, unimodality of the strong sense does not appear in the case of $\alpha = 0$. We tested other values of α, too. If $-3 < \alpha < -2.38$ there was no bifurcation from the trivial solutions. Based on

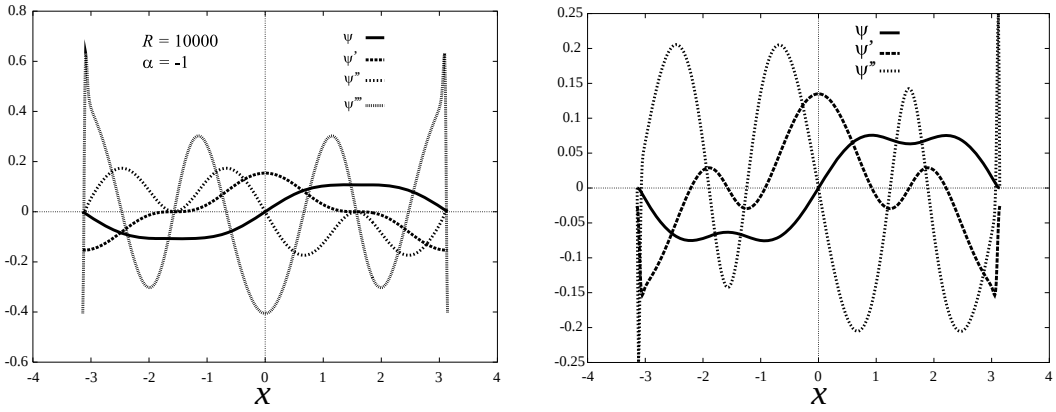

Figure 19: Graphs of $\psi, \psi', \psi'', \psi'''$. $\ell = 2$. $\alpha = -1, R = 10^4$(left). Graphs of ψ, ψ', ψ''. $\ell = 2$. $\alpha = -2, R = 10^4$(right).

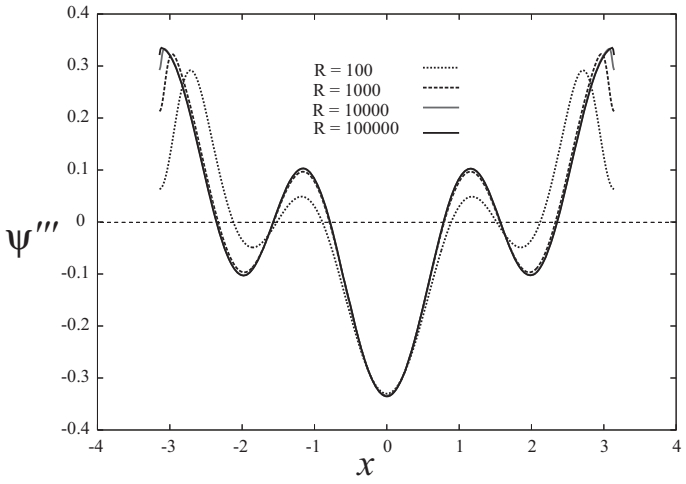

Figure 20: Graphs of the bifurcating solutions. ψ''' are plotted. $\ell = 2$. $\alpha = 0$. Solutions with $R = 100, 1000, 10^4, 10^5$ are shown.

these experiments for values of $\alpha \in (-3, 1)$, we conclude that unimodality of strong sense does not appear if $-3 < \alpha < 1$.

6 The case of $\alpha = -3$

We prove in this section that the bifurcation does not exist if $\alpha = -3$. We set $\alpha = -3$ in (1.1) and integrate it twice to obtain

$$\psi_t + \psi\psi_x = \frac{1}{R}\left(\psi_{xx} + \frac{1}{\ell^2}\sin \ell x + \frac{R}{2\ell^7}\sin 2\ell x\right).$$

We then set $\psi(t, x) = \ell^{-4}u(\ell^{-4}t, x)$ and $R' = R\ell^{-4}$. The result is:

$$u_\tau = \frac{1}{R'}u_{xx} - uu_x + \frac{1}{R'}\ell^2 \sin \ell x + \frac{\ell}{2}\sin 2\ell x,$$

where $\tau = \ell^{-4}t$. Let t and R denote τ and R', respectively. Our equation is then

$$u_t = \frac{1}{R}u_{xx} - uu_x + \frac{1}{R}\ell^2 \sin \ell x + \frac{\ell}{2}\sin 2\ell x \qquad (-\pi < x < \pi), \tag{6.1}$$

where the periodic boundary condition is imposed. Clearly $u = \sin \ell x$ is a solution, whose stability we are going to prove.

We now set $u = \sin \ell x + v$ in (6.1) and linearize with respect to v to obtain

$$v_t = \frac{1}{R}v_{xx} - (v \sin \ell x)_x. \tag{6.2}$$

By restricting ourselves to odd solutions in x, we may consider (6.2) in $0 < x < \pi$ with

$$v(0) = v(\pi) = 0. \tag{6.3}$$

Theorem 6.1 *If $\ell = 1$, then every solution of (6.2) and (6.3) tends to zero. For a general ℓ, any stationary solution of (6.2) and (6.3) is identically zero.*

Proof. Suppose that $\ell = 1$. We multiply (6.2) by $v(x)\sin x$ and integrate it in $0 < x < \pi$. We then obtain

$$\begin{aligned}\frac{1}{2}\frac{\mathrm{d}}{\mathrm{d}t}\int_0^\pi v(t,x)^2 \sin x \,\mathrm{d}x &= \int_0^\pi vv_t \sin x \,\mathrm{d}x = -\frac{1}{R}\int_0^\pi v_x(v\sin x)_x \\ &= -\frac{1}{R}\int_0^\pi v_x^2 \sin x \,\mathrm{d}x - \frac{1}{R}\int_0^\pi v_x v \cos x \,\mathrm{d}x \\ &= -\frac{1}{R}\int_0^\pi v_x^2 \sin(x) \,\mathrm{d}x - \frac{1}{2R}\int_0^\pi v^2 \sin x \,\mathrm{d}x.\end{aligned}$$

We therefore have

$$\frac{\mathrm{d}}{\mathrm{d}t}I(t) \le -\frac{1}{R}I(t), \quad \text{where} \quad I(t) = \int_0^\pi v(t,x)^2 \sin x \,\mathrm{d}x.$$

Accordingly, $\int_0^\pi v^2 \sin x \,\mathrm{d}x$ decays exponentially to zero as $t \to \infty$. Starting with this estimate, we may successively prove that other integrals such as $\int v^2, \int v_x^2, \cdots$ tends to zero as $t \to \infty$.

We now suppose that ℓ is a positive integer and that v is independent of t. Then,

$$\frac{1}{R}v_x - v\sin \ell x = c,$$

where c is a constant. We can solve this equation by the method of variation of parameters: Set

$$v(x) = A(x)\exp\left(-\frac{R}{\ell}\cos \ell x\right).$$

We then have

$$A'(x) = cR\exp\left(\frac{R}{\ell}\cos \ell x\right).$$

Since $v(0) = 0$, we obtain

$$v(x) = cR\int_0^x \exp\left(-\frac{R}{\ell}\cos \ell x + \frac{R}{\ell}\cos \ell y\right)\,\mathrm{d}y.$$

This must satisfy $v(\pi) = 0$ by the boundary condition. We see easily that it is the case if and only if $c = 0$. Namely, $v \equiv 0$. ∎

This theorem implies that for $\ell \ge 2$, there is no bifurcation of odd steady-state. If $\ell = 1$, then no bifurcation, steady or Hopf, exists among the odd functions. However, we cannot exclude the possibility of Hopf bifurcation if $\ell \ge 2$.

7 Cases where $\alpha < -3$

As Figure 8 indicates, there are bifurcation points in the range $\alpha < -3$. Let us see what is happening in this range of α.

Bifurcation diagrams at $\alpha = -3.2$ and $\alpha = -4.4$ are drawn in Figure 21. If $\alpha = -3.2$ the diagram is disconnected into upper and lower branches, while if $\alpha = -4.4$, it is separated into left and right branches. The right one is a 'hairpin' curve. In each case, there exists a family of solutions where R increases indefinitely to ∞ and those where R decreases to zero.

We now examine that unimodality is not observed in those solutions of increasing R. When $\alpha = -3.2$, there are two solutions with very large R. The graphs of ψ' are plotted in Figure 22, where two solutions are very close to each other except in the boundary layer

near $x = \pm\pi$. Similarly we computed solutions with large R with different α. As far as we computed for $-40 < \alpha < -3$, no unimodality was observed at all. We also verified that the solutions with $a_1 \uparrow$ and $R \downarrow 0$ show no unimodality (figures are omitted).

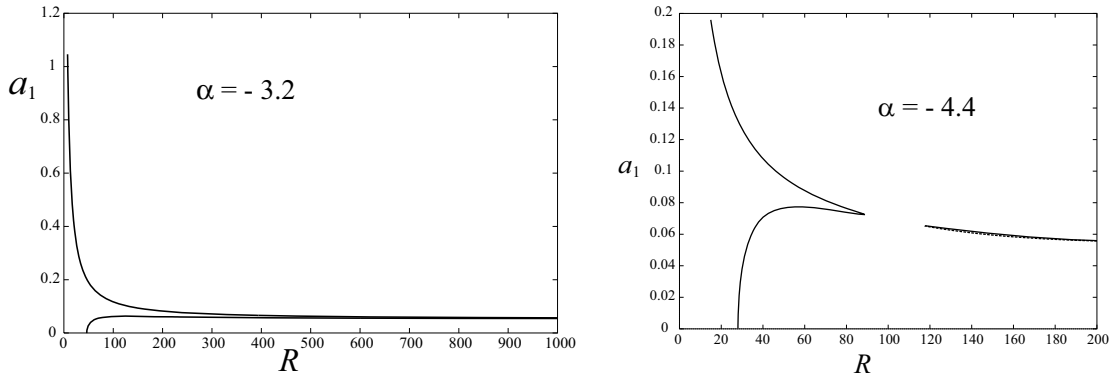

Figure 21: Bifurcation diagrams for $\alpha = -3.2$ (left) and $\alpha = -4.4$ (right). $\ell = 2$. Critical Reynolds numbers are approximately 46.31 and 28.01, respectively. Only those parts of $a_1 > 0$ are plotted because of the symmetry.

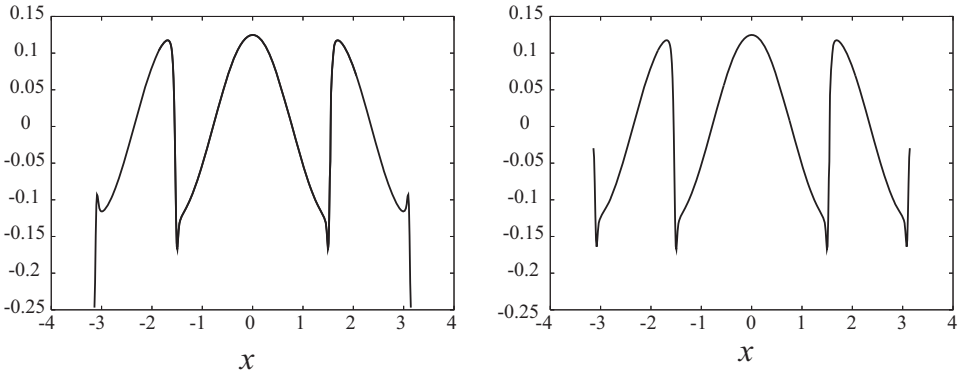

Figure 22: Graphs of two different ψ'. $R = 10^4, \alpha = -3.2$.

8 Stability

In this section we prove some facts on the neutral curves. In Kim & Okamoto (2010) we proved that the steady-state $\ell^{-4} \sin \ell x$ is stable for all $R > 0$ if $\ell = 1$. We also proved that, if $\ell = 2$, a bifurcation of steady-states occurs at $R = R_c$, where $3.55 < R_c < 3.5971$. These results were, however, only for the case of $\alpha = 1$. Accordingly we study here the same problem for general α. In particular, we prove that there is no bifurcation of odd stationary solutions if $\ell = 1$ and $-7/2 \leq \alpha \leq 1$.

Following Iudovich (1965), Kim & Okamoto (2010), and Meshalkin & Sinai (1962), let us set now $\psi = \ell^{-4}\sin\ell x + g$, substitute it into (1.1), and linearize in g. We then obtain

$$g_{txx} + \frac{\sin\ell x}{\ell^2}\left(\alpha g_x + \ell^{-2} g_{xxx}\right) - \frac{\cos\ell x}{\ell}\left(g + \ell^{-2}\alpha g_{xx}\right) = R^{-1} g_{xxxx}. \tag{8.1}$$

Substituting $g(x,t) = e^{\lambda t}\sum_{n=1}^{\infty} c_n \sin nx$ into (8.1), we have the following recurrence relation for $n \geq 1$,

$$2n\left(\lambda + \frac{n^2}{R}\right)\ell^4 c_n + A(n,\alpha,\ell)\, c_{n-\ell} - B(n,\alpha,\ell)\, c_{n+\ell} = 0, \tag{8.2}$$

where $A(n,\alpha,\ell) = (n-2\ell)^2 + (1-\alpha)\ell(n-\ell)$ and $B(n,\alpha,\ell) = (n+2\ell)^2 + (\alpha-1)\ell(n+\ell)$, and we have set $c_0 = 0$ and $c_{-j} = -c_j$ for $j = 1, 2, \cdots, \ell-1$. For later discussion, we note the positivity of the coefficients $A(n,\alpha,\ell)$ and $B(n,\alpha,\ell)$:

Lemma 8.1 *Suppose that $\ell \geq 1$, $-3 \leq \alpha \leq 1$, and $n \geq 1$. Then $A(n,\alpha,\ell) \geq 0$ and $B(n,\alpha,\ell) > 0$. The equality holds true if and only if $\alpha = 1$ and $n = 2\ell$. If $\ell = 1$, then the same conclusion holds for all $-7/2 < \alpha \leq 1$.*

Proof. Note that

$$A(n,\alpha,\ell) = \left(n - \frac{\ell(3+\alpha)}{2}\right)^2 + \frac{\ell^2(3+\alpha)(1-\alpha)}{4},$$
$$B(n,\alpha,\ell) = \left(n + \frac{\ell(3+\alpha)}{2}\right)^2 + \frac{\ell^2(3+\alpha)(1-\alpha)}{4},$$

which implies the first conclusion. The second conclusion is proved similarly, because of $A(n,\alpha,1) = n^2 - (\alpha+3)n + \alpha + 3$ and $B(n,\alpha,1) = n^2 + (\alpha+3)n + \alpha + 3$. ∎

We first consider the case where $\ell = 1$. The following theorem asserts that there is no eigenvalue λ of nonnegative real part for $-7/2 \leq \alpha \leq 1$. In particular, the trivial solution with $\ell = 1$ is stable for all the Reynolds numbers if $-7/2 \leq \alpha \leq 1$.

Theorem 8.1 *Suppose that $\ell = 1$ and that $\Re[\lambda] \geq 0$. Then $c_n \equiv 0$ is the only solution of (8.2) for all $-7/2 \leq \alpha \leq 1$ and $0 < R < \infty$.*

Proof. We first note that we consider only those solutions of (8.2) such that $\sum_n |c_n|^2 < \infty$. We next note the following proposition: if there exists a non-trivial solution with $\Re[\lambda] \geq 0$, then λ is real. This can be proved just as Meshalkin and Sinai proved a similar proposition for Kolmogorov flow. See Meshalkin & Sinai (1962). We omit the details.

By this proposition we henceforth assume that λ is a non-negative real number. We accordingly assume that c_n's are real, too. We now prove that $c_n \neq 0$ for all $n \geq 1$ unless c_n's are identically zero. Since $c_0 = 0$, $c_1 = 0$ implies $c_2 = 0$. Applying the same argument

repeatedly, we conclude that $c_1 \neq 0$ unless $c_n \equiv 0$. Suppose now that there exists a k such that $c_1 \neq 0, c_2 \neq 0, \cdots, c_k \neq 0$ and $c_{k+1} = 0$. Then the recurrence relation closes in $c_1, c_2, \cdots, c_k$ only. This relation can be written as

$$M \begin{pmatrix} c_1 \\ c_2 \\ \vdots \\ c_k \end{pmatrix} = \begin{pmatrix} 0 \\ 0 \\ \vdots \\ 0 \end{pmatrix},$$

where the matrix M is of the following tri-diagonal form:

$$M = \begin{pmatrix} q_1 & -B(1) & 0 & 0 & \cdots & 0 \\ A(2) & q_2 & -B(2) & 0 & \cdots & 0 \\ 0 & A(3) & q_3 & -B(3) & \cdots & 0 \\ \vdots & \vdots & & \ddots & & \vdots \\ 0 & \cdots & 0 & A(k-1) & q_{k-1} & -B(k-1) \\ 0 & \cdots & 0 & 0 & A(k) & q_k \end{pmatrix},$$

where $A(k)$ and $B(k)$ denote $A(k, \alpha, 1)$ and $B(k, \alpha, 1)$, respectively and $q_n = 2n(\lambda + n^2/R)$ $(n = 1, 2, \cdots, k)$. M is easily seen to be nonsingular. Hence our claim follows.

Suppose next that we have a solution $\{c_n\} \neq \{0\}$. We may then introduce $\rho_n = c_n/c_{n-1}$ for $n > 1$ and simplify (8.2) as

$$\frac{2n}{B(n, \alpha, 1)} \left(\lambda + \frac{n^2}{R} \right) + \frac{A(n, \alpha, 1)}{B(n, \alpha, 1)\rho_n} = \rho_{n+1}. \tag{8.3}$$

Now from (8.2) for $n = 1$ we have

$$2(\lambda + 1/R)c_1 - (2\alpha + 7)c_2 = 0.$$

If $\alpha = -7/2$, then $c_1 = 0$, whence $c_n = 0$ for all n. We now suppose that $-7/2 < \alpha$. We then obtain

$$\rho_2 = \frac{c_2}{c_1} = \frac{2}{2\alpha + 7} \left(\lambda + \frac{1}{R} \right) \geq \frac{2}{(2\alpha + 7)R} \geq \frac{2}{9R}$$

for all $-7/2 < \alpha \leq 1$. Thus, applying a mathematical induction to (8.3), we deduce $\rho_n > 0$ for all $n > 1$. Moreover, since $B(n, \alpha, 1) \leq (n + 2)^2$, it follows, by (8.3) again, that

$$\rho_{n+1} > \frac{2n^3}{B(n, \alpha, 1)} \frac{1}{R} \geq \frac{2n^3}{(n + 2)^2 R} \geq \frac{n}{2R} \tag{8.4}$$

for all $n > 1$, which implies

$$|c_n| = |c_1||\rho_2 \cdots \rho_n| \geq |c_1| \frac{2}{9R} \left(\frac{1}{2R} \right)^{n-2} (n - 1)!.$$

The right hand side tends to infinity as $n \to \infty$ for each fixed $R > 0$ and $-7/2 < \alpha \leq 1$. Thus the Fourier series is divergent. Consequently, $c_n \equiv 0$ is the only solution. ∎

We next consider the case where $\ell = 2$. Henceforth we assume that $-3 \leq \alpha \leq 1$. The recurrence relation reads

$$2^5 n \left(\lambda + \frac{n^2}{R}\right) c_n + A(n,\alpha,2)c_{n-2} - B(n,\alpha,2)c_{n+2} = 0 \qquad (1 \leq n) \tag{8.5}$$

with $c_0 = 0$ and $c_{-1} = -c_1$. For the sake of convenience, we define c_n for $n = -2, -3, \cdots$, by requiring that (8.5) holds for all integer n. The well-definedness of c_n comes from Lemma 8.1. (8.5) shows that the coefficients c_{2k-1} with odd indices are related each other but are independent of the coefficients c_{2k} with even indices. We first prove that $c_2 = c_4 = \cdots = 0$. We set $n = 2k$ in (8.2) and rewrite it with $c'_k = c_{2k}$. Then we have

$$2^4 k \left(\lambda + \frac{4k^2}{R}\right) c'_k + [(k-2)^2 + (1-\alpha)(k-1)]c'_{k-1} - [(k+2)^2 + (\alpha-1)(k+1)]c'_{k+1} = 0 \qquad (1 \leq k)$$

and $c'_0 = 0$. This is the same as the recurrence formula (8.2) in the case of $\ell = 1$, except for a change in the coefficient of c'_k. We may apply the same argument and conclude that c'_k is zero for all k. The details are left to the reader.

For the odd coefficients, the recurrence relation becomes

$$2^5(2k+1)\left(\lambda + \frac{(2k+1)^2}{R}\right) c_{2k+1} + A(2k+1)c_{2k-1} - B(2k+1)c_{2k+3} = 0 \qquad (0 \leq k), \tag{8.6}$$

where $A(2k+1) = (2k-3)^2 + 2(1-\alpha)(2k-1)$ and $B(2k+1) = (2k+5)^2 + 2(\alpha-1)(2k+3)$, both of which are positive for all $-3 \leq \alpha \leq 1$. In the same way as before, we may conclude that either all of them are zero or none of them is zero.

Suppose that $\{c_{2k-1}\}$ is a non-trivial solution. Then we may introduce $\rho_n = c_{2n+1}/c_{2n-1}$ for $n \in \mathbb{Z}$ and rewrite (8.6) as

$$a_{2n+1} + D(2n+1)\frac{1}{\rho_n} = \rho_{n+1}, \tag{8.7}$$

where $a_n = \frac{2^5 n}{B(n)}(\lambda + \frac{n^2}{R})$ and $D(n) = \frac{A(n)}{B(n)}$. Then for all n the following relation holds true:

$$\rho_n = a_{2n-1} + \cfrac{D(2n-1)}{a_{2n-3} + \cfrac{D(2n-3)}{a_{2n-5} + \cfrac{D(2n-5)}{\ddots}}} = -\cfrac{D(2n+1)}{a_{2n+1} + \cfrac{D(2n+3)}{a_{2n+3} + \cfrac{D(2n+5)}{\ddots}}}. \tag{8.8}$$

This is a necessary condition for a non-trivial solution to exist. We now note

Proposition 8.1 *Suppose that for some n_0 we have*

$$a_{2n_0-1}+\cfrac{D(2n_0-1)}{a_{2n_0-3}+\cfrac{D(2n_0-3)}{a_{2n_0-5}+\cfrac{D(2n_0-5)}{\ddots}}}=-\cfrac{D(2n_0+1)}{a_{2n_0+1}+\cfrac{D(2n_0+3)}{a_{2n_0+3}+\cfrac{D(2n_0+5)}{\ddots}}}. \tag{8.9}$$

We then define ρ_{n_0} as this quantity. For other n, we define ρ_n by (8.7). With this $\{\rho_n\}$, we define $\{c_n\}$ by $\rho_n = c_{2n+1}/c_{2n-1}$. We can define $\{c_n\}$ uniquely if we set $c_1 = 1$.

The proof of this proposition is the same as in the case of $\alpha = 1$ in Kim & Okamoto (2010), which utilizes the idea of Iudovich (1965) and Meshalkin & Sinai (1962). Since the proof is straightforward, we omit it.

Let us now set $n = 0$ to obtain

$$a_{-1}+\cfrac{D(-1)}{a_{-3}+\cfrac{D(-3)}{a_{-5}+\cfrac{D(-5)}{\ddots}}}=-\cfrac{D(1)}{a_1+\cfrac{D(3)}{a_3+\cfrac{D(5)}{\ddots}}}. \tag{8.10}$$

We now prove that there exists an $R > 0$ for which (8.10) holds true. Let $f(\lambda, R, \alpha)$ denote the denominator of the right hand side. Since

$$a_{-(2n-1)} = -\frac{1}{D(2n-1)}a_{2n-1}$$

and

$$A(n) = B(-n), \quad B(n) = A(-n) \quad (n \geq 1)$$

we may rewrite (8.10) as

$$-\frac{1}{D(1)}f(\lambda, R, \alpha) = -\frac{D(1)}{f(\lambda, R, \alpha)} \tag{8.11}$$

which, together with $\mathrm{Re}[\lambda] \geq 0$, implies that

$$f(\lambda, R, \alpha) = \frac{A(1)}{B(1)} = \frac{2\alpha+7}{6\alpha+19}. \tag{8.12}$$

This is the equation which determines the critical Reynolds number.

Let us now suppose that $\lambda = 0$. Since $f(0, R, \alpha) > a_1 = \frac{32}{(6\alpha+19)R}$, we see that

$$\lim_{R\to 0} f(0, R, \alpha) = +\infty,$$

if $\alpha > -19/6$ which is the current case. On the other hand we see that

$$f(0, R, \alpha) < a_1 + \frac{D(3)}{a_3} = \frac{32}{(6\alpha+19)R} + \frac{(3-2\alpha)R}{2^5 \cdot 3^3}.$$

If the right hand side with $R = 16$ is smaller than $\frac{2\alpha+7}{6\alpha+19}$, then (8.12) must have a root in $0 < R < 16$. It is not difficult to show that this is indeed the case if $12\alpha^2 + 128\alpha + 213 > 0$, namely if $\alpha > (\sqrt{385} - 32)/6 = -2.06\cdots$. But it is not easy to see precisely how small α can be for (8.12) to have a root.

If we consider only the first part of the continued fraction expression of $f(0, R, \alpha)$, we have an estimate

$$\frac{32}{(6\alpha + 19)R} < \frac{2\alpha + 7}{6\alpha + 19}. \tag{8.13}$$

This yields

$$R > \frac{32}{2\alpha + 7}.$$

We proceed to the next order approximation to have

$$\frac{32}{(6\alpha + 19)R} + \frac{(3 - 2\alpha)R}{32 \cdot 27} > \frac{2\alpha + 7}{6\alpha + 19}. \tag{8.14}$$

This implies that either

$$R > \frac{48\left(18\alpha + 63 + \sqrt{468\alpha^2 + 2508\alpha + 3285}\right)}{57 - 20\alpha - 12\alpha^2}$$

or

$$R < \frac{48\left(18\alpha + 63 - \sqrt{468\alpha^2 + 2508\alpha + 3285}\right)}{57 - 20\alpha - 12\alpha^2}$$

if the expression inside the square root is positive, i.e., $\alpha > \alpha_0 = -2.278961555\cdots$. Combining this with the first order approximation, we obtain upper and lower bounds for the critical Reynolds number:

$$\frac{32}{2\alpha + 7} < R_c < \frac{-48(18\alpha + 63 - \sqrt{468\alpha^2 + 2508\alpha + 3285})}{-57 + 20\alpha + 12\alpha^2}$$

for $\alpha_0 < \alpha \leq 1$. If we go one step further to obtain the third order approximation, then we have more accurate bounds. The results are depicted for each fixed α as two curves representing the second order approximation (upper) and the third order approximation (lower) in Figure 23. Numerical results are displayed by + marks, which obviously are very close to the upper curve (i.e. the second order approximation), showing a good agreement.

Near the point $\alpha_0 = -2.278961555...$ the second order approximation no longer permits a real positive critical Reynolds number. But this only shows that the approximation is no longer a good one. Nor does it imply the absence of bifurcation for those α smaller than α_0. In fact, Figure 14 shows that bifurcation exists even in $\alpha = -2.36$. If we assume that the critical Reynolds number exists and if we solve the third order approximation, it provides us an approximate critical Reynolds number for all $-3 \leq \alpha \leq 1$. However, the third order approximation is not good enough to suggest a behaviour of the neutral curve (the (α, R) curve of the critical Reynolds numbers).

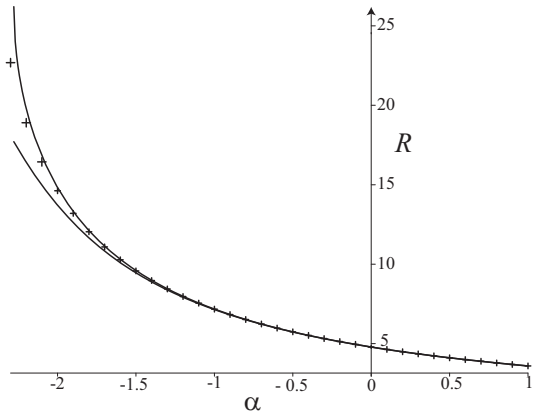

Figure 23: Upper and lower bounds for the critical Reynolds numbers. ('+' represents the numerical result).

9 Conclusions

Our computation shows that the solutions become strongly unimodal if and only if $\alpha = 1$ and $R \to \infty$. This conforms to our conjecture that unimodal solutions at $1 \ll R$ is connected to the 2D Navier-Stokes equation. Strongly unimodal solutions do not appear if $1 < \alpha$. On the other hand, weakly unimodal solutions were found in $-2.3\cdots < \alpha < 1$. We also found some solutions which become very large as $R \downarrow 0$. The global bifurcation diagram with varying (α, R) is complicated, and we will report on their structures in the forthcoming paper.

Some of the asymptotic properties of the solution as $R \to \infty$ are shown to agree with the result by the asymptotic expansion. Theoretical prediction about the neutral curve matches well for $-2 < \alpha$.

10 Appendix: A case of a different force

The purpose of the present section is to give an example of an external force of a single term. We actually consider

$$\psi_{txx} + \psi\psi_{xxx} - \alpha\psi_x\psi_{xx} = \frac{1}{R}\left(\psi_{xxxx} - \sin 5x\right), \tag{10.1}$$

where 5 was chosen just arbitrarily. Similar results can be obtained for $f = \sin 4x$ and $f = \sin 6x$. For the sake of simplicity only those results for $\alpha = 0$ are presented.

Since no explicit solution is available in this case, we start with $\psi = 5^{-4}\sin 5x$ which is a good approximation if R is small enough. We then apply the path-continuation method and increase R gradually. We obtain Figure 24 (left) as a bifurcation diagram. The branch

which is denoted by the broken line consists of those solutions represented as

$$\psi(x) = a_5 \sin 5x + a_{10} \sin 10x + a_{15} \sin 15x + \cdots .$$

We call it the main branch. The graphs are plotted in Figure 24 (right). The solutions on the secondary branch which bifurcate at $R \approx 275$ have non-zero values in a_1 (and others). Their graphs are shown in Figure 25. If R is increased further, the peak at $x = \pm\pi$ becomes higher and the interior layer at $x = \pm$ becomes thinner. But the other undulations remain. These are graphs of ψ'''. The graphs of ψ show that they are unimodal. So we obtain weakly unimodal solutions similar to those in the previous forcing case.

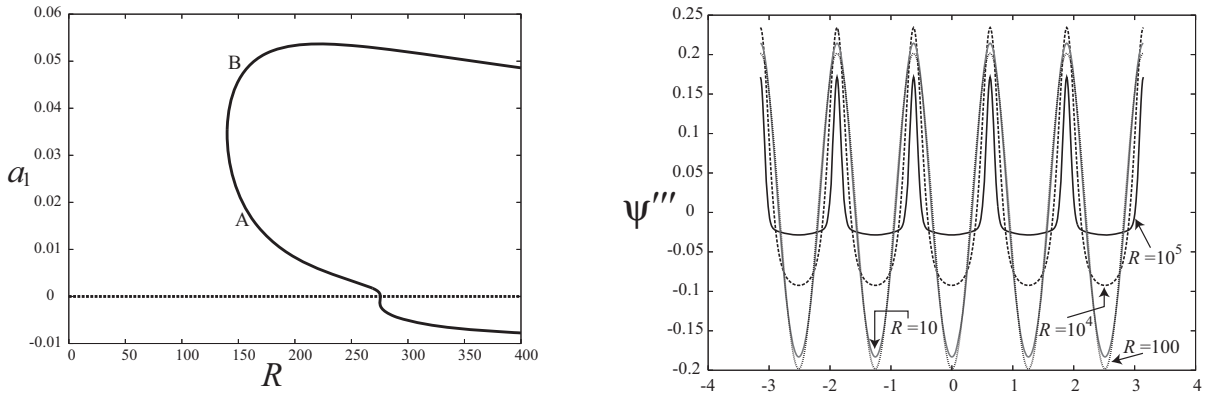

Figure 24: Bifurcation diagrams (left). Graphs of solutions on the main branch (right). $f = \sin 5x$; $\alpha = 0$.

Funding. SCK is supported by Basic Science Research Program through the National Research Foundation of Korea funded by the Ministry of Education, Science and Technology(2010-0007654). HO is partially supported by JSPS Grant 20244006.

References

[1] Budd, C., Dold, B., & Stuart, A., (1993) Blowup in a partial differential equation with conserved first integral, *SIAM J. Appl. Math.*, **53**, 718–742.

[2] Budd, C., Dold, B., & Stuart, A. (1994), Blowup in a system of partial differential equations with conserved first integral. Part II: Problems with convection, *SIAM J. Appl. Math.*, **54**, 610–640.

[3] Chen, X. & Okamoto, H. (2002), Global Existence of Solutions to the generalized Proudman–Johnson Equation, *Proc. Japan Acad.*, **78**, 136–139.

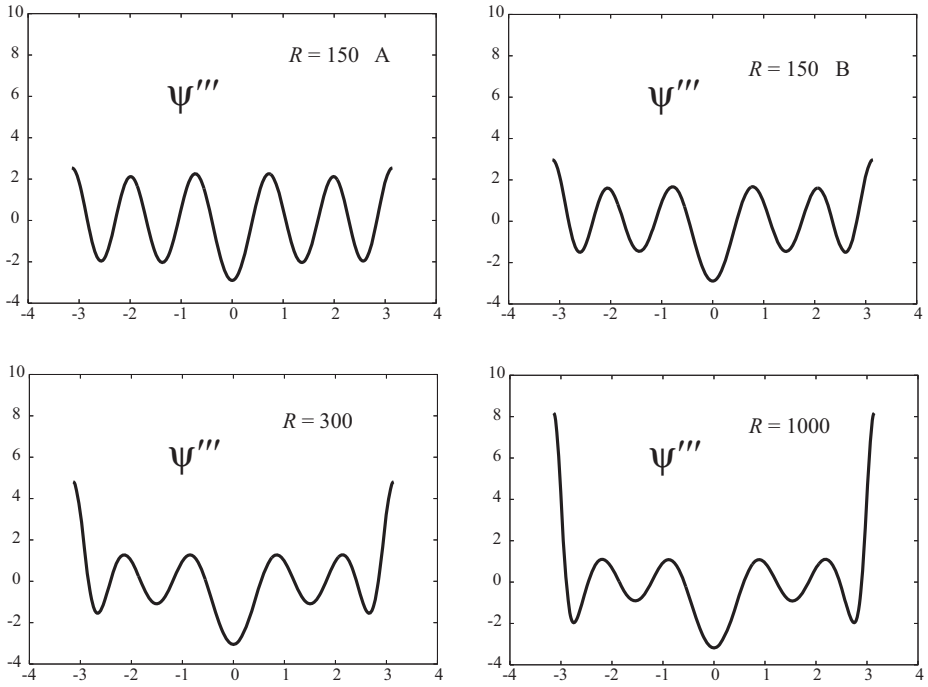

Figure 25: Graphs of solutions on the upper secondary branch. $\alpha = 0$. $f = \sin 5x$. The letters A and B imply that the solution corresponds to that labeled as such in Figure 24 (left).

[4] Cho, C.-H. & Wunsch, M., Global and singular solutions to the generalized Proudman.Johnson equation, *J. Diff. Eq.*, **249** (2010), 392–413.

[5] Cox, S. M. (1991), Analysis of steady flow in a channel with one porous wall, or with accelerating walls, *SIAM J. Appl. Math.* **51**, 429–438.

[6] Cox, S. M. (1991a), Two-dimensional flow of a viscous fluid in a channel with porous walls, *J. Fluid Mech.*, **227**, 1-33.

[7] Grundy, R. E. & McLaughlin, R. (1997), Global blow-up of separable solutions of the vorticity equation, *IMA J. Appl. Math.*, **59**, 287–307.

[8] Grundy, R. E. & McLaughlin, R. (1999), Three-dimensional blow-up solutions of the Navier-Stokes equations, *IMA J. Appl. Math.*, **63**, 287–306.

[9] Holm, D.D. & , Hone, A.N.W. (2008), A class of equations with peakon and pulson solutions (with an Appendix by Harry Braden and John Byatt-Smith), arXiv:nlin/0412029v1.

[10] Hunter, J. K. & Saxton, R. (1991), Dynamics of director fields, *SIAM J. Appl. Math.*, **51**, 1498–1521.

[11] Ikeda, H., Kondo, K., Okamoto, H. & Yotsutani, S. (2003), On the global branches of the solutions to a nonlocal boundary-value problem arising in Oseen's spiral flows, *Commun. Pure Appl. Anal.*, **2**, 373–382.

[12] Ikeda, H., Mimura, M. & Okamoto, H. (2001), A singular perturbation problem arising in Oseen's spiral flows, *Japan J. Indust. Appl. Math.*, **18**, 393–403.

[13] Iudovich, V.I. (1965), Example of the generation of a secondary stationary or periodic flow when there is loss of stability of the laminar flow of a viscous incompressible fluid, *J. Appl. Math. Mech.*, **29**, 527–544.

[14] Kim, S.-C. & Okamoto, H. (2003), Bifurcations and inviscid limit of rhombic Navier-Stokes flows in tori, *IMA J. Appl. Math.*, **68**, 119–134.

[15] Kim, S.-C. & Okamoto, H. (2010), Vortices of large scale appearing in 2D stationary Navier-Stokes equations at large Reynolds numbers, *Japan J. Indus. Appl. Math.*, **27** 47–71.

[16] Meshalkin, L. D. & Sinai, Y.G. (1962), Investigation of the stability of a stationary solution of a system of equations for the plane movement of an incompressible viscous liquid, *J. Appl. Math. Mech.*, **25**, 1700-1705.

[17] Okamoto, H. (2009), Well-posedness of the generalized Proudman-Johnson equation without viscosity, *J. Math. Fluid Mech.* **1**, 46–59.

[18] Okamoto, H. & Zhu J. (2000), Some similarity solutions of the Navier-Stokes equations and related topics, *Taiwanese J. Math.*, **4**, 65–103.

[19] Proudman, I. & Johnson, K. (1962), Boundary-layer growth near a rear stagnation point, *J. Fluid Mech.*, **12**, 161–168.

[20] Riabouchinsky, D., Quelques considérations sur les mouvements plans rotationnels d'un liquide, *Comp. Rend. Acad. Sci. Paris*, **179** (1924), 1133–1136.

[21] Saxton, R. and Tiğlay, F., Global existence of some infinite energy solutions for a periodic incompressible fluid, *SIAM J. Math. Anal.*, **40**, (2008), 1499–1515.